Planetary and Space Science 153 (2018) 107–119

Contents lists available at ScienceDirect

Planetary and Space Science

journal homepage: www.elsevier.com/locate/pss

A high-performance electric field detector for space missions

D. Badoni [a,b,*], R. Ammendola [a], I. Bertello [c], P. Cipollone [a], L. Conti [d,a], C. De Santis [a], P. Diego [c], G. Masciantonio [a], P. Picozza [b,a], R. Sparvoli [b,a], P. Ubertini [c], G. Vannaroni [c,d]

[a] INFN Sezione di Roma Tor Vergata, Via della Ricerca Scientifica 1, I-00133 Rome, Italy
[b] Department of Physics, University of Rome 'Tor Vergata', Via della Ricerca Scientifica 1, I-00133 Rome, Italy
[c] INAF-IAPS, Via del Fosso del Cavaliere 100, I-00133 Rome, Italy
[d] Uninettuno University, Corso Vittorio Emanuele II, 39, I-00186 Rome, Italy

ARTICLE INFO

Keywords:
Electric field detector
Satellite instruments
Magnetosphere
Ionosphere
Earthquake
Electromagnetic emissions

ABSTRACT

We present the prototype of an Electric Field Detector (EFD) for space applications, that has been developed in the framework of the Chinese-Italian collaboration on the CSES (China Seismo-Electromagnetic Satellite) forthcoming missions. In particular CSES-1 will be placed in orbit in the early 2018. The detector consists of spherical probes designed to be installed at the tips of four booms deployed from a 3-axes stabilized satellite. The instrument has been conceived for space-borne measurements of electromagnetic phenomena such as ionospheric waves, lithosphere-atmosphere-ionosphere-magnetosphere coupling and anthropogenic electromagnetic emissions. The detector allows to measure electric fields in a wide band of frequencies extending from quasi-DC up to about 4 *MHz*, with a sensitivity of the order of $1\mu V/m$ in the ULF band. With these bandwidth and sensitivity, the described electric field detector represents a very performing and updated device for electric field measurements in space.

1. Introduction

The lithosphere-atmosphere-ionosphere-magnetosphere coupling involves a lot of physical effects and interactions at all levels starting from underground up to the Earth's magnetosphere. Seismicity is a source of electromagnetic signals at ground and in the near-Earth space (Pulinets and Boyarchuk, 2005). Even not exhaustive, a review of some measurements and related analyses on ground and space based data of possible seismic precursors can be found in Rodger et al. (1999) and in Tables 2 and 3 of Sgrigna and Conti (2012). Early analyses have correlated some ULF anomalies detected on ground with earthquakes (such as the strong Loma Prieta event of 1989 (Fraser-Smith et al., 1990). Although these results have been intensely debated (Fraser-Smith et al. (2011); Campbell (2009) and Fraser-Smith et al. (2011)), the low frequency band is one of the most interesting for investigating seismo-electromagnetic signals due to the lower attenuation induced by the lithosphere-atmosphere-ionosphere layers. Nevertheless, in the case of very shallow and strong earthquakes, when the size of the preparation focal zone is greater than the hypo-central depth, also the higher frequency signals could be transmitted on ground and to the near space (Sgrigna et al., 2004).

Some slow electro-telluric and magnetic field variations (Varotsos and Alexopoulos, 1984a), (Varotsos and Alexopoulos, 1984b) as well as ULF emissions (Fraser-Smith et al., 1990); (Molchanov et al., 1995); (Kopytenko et al., 1993), ELF-VLF disturbances (Gokhberg et al., 1982), (Fujinawa and Takahashi, 1998), and HF emissions (Warwick et al., 1982) have been correlated with the occurrence of earthquakes. Some observations of electric and magnetic field fluctuations in the frequency range $10Hz - 15kHz$ obtained by satellite AUREOL-3 (Parrot, 1989) have been claimed to be short-term seismic precursors. Perturbations in the ULF/ELF/VLF bands have been detected before earthquakes by the ITK1300 and the Intercosmos-24 satellites several hours before the main shock (Molchanov et al., 1993). The most recent satellite studies of seismo-associated electromagnetic and ionospheric phenomena have been performed by the French satellite Demeter (nearly Sun-synchronous orbit at an altitude of about 700 *km*). ICE, the Demeter electric field detector, has the sensitivity in ELF (at the frequencies above 100 Hz)/VLF/HF bands and resolution in ULF (quasi-DC) band of 0.1 $\frac{\mu V}{m\cdot\sqrt{Hz}}$, 0.05 $\frac{\mu V}{m\cdot\sqrt{Hz}}$, 0.1 $\frac{\mu V}{m\cdot\sqrt{Hz}}$ and 40 $\frac{\mu V}{m}$ respectively (Berthelier et al., 2006). In this framework, several statistical analyses (Piša et al. (2012); Němec et al. (2008), Piša et al. (2012, 2013)) of about 1 – 2 kHz electric field data (gathered by ICE), show that the normalized intensity of the

* Corresponding author. INFN Sezione di Roma Tor Vergata, Via della Ricerca Scientifica 1, I-00133 Rome, Italy.
E-mail address: davide.badoni@roma2.infn.it (D. Badoni).

https://doi.org/10.1016/j.pss.2018.01.013
Received 26 July 2017; Received in revised form 25 January 2018; Accepted 29 January 2018
Available online 5 February 2018
0032-0633/

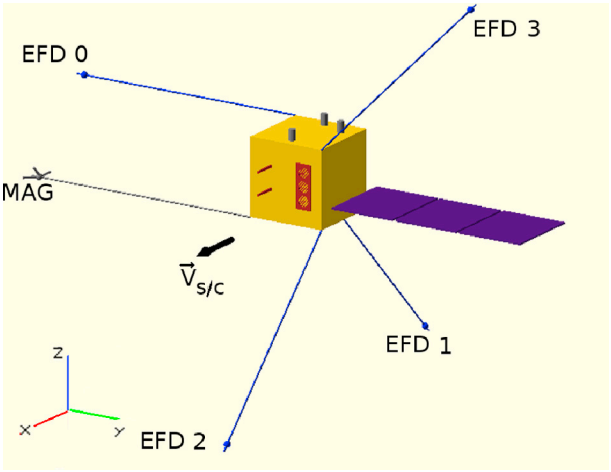

Fig. 1. Positioning of the EFD sensor (0, 1, 2 and 3) on the satellite booms. The x axis is parallel to S/C motion, z is to zenit and y completes the orthogonal reference system.

night-time electric field amplitude decreases below the mean background level few hours (0–4 h) before the shallow (depth $<$ 40 km) of medium and strong ($M > 5$) earthquakes. The spatial scale of the affected area (about 350 km) is in good agreement with the size r of the preparation zone for earthquakes of magnitude $M > 5$ estimated with the Dobrovolsky et al. (1979) formula $r = 10^{0.43\,M}\ km$. A possible explanation of the observed perturbation is a local lowering of the ionosphere bottom layer induced by seismo-associated phenomena. Significantly, the largest decrease occurs at about 1.7 kHz, i.e. approximately near to the cut-off frequency of the first transverse magnetic mode of the Earth-ionosphere waveguide in night-time. An increase of this cut-off frequency would induce a decrease of the electric field power spectral density (as statistically observed by Demeter) and an increase of the plasma density in the lower ionosphere above the earthquakes preparation area. This will result into a local perturbation of the propagation of whistlers, which are the main natural electromagnetic waves propagating in the Earth-ionosphere wave-guide. Anyway, at present, there is not clear evidence of the precursors signature (i.e. in which range and condition a detected signal can be considered anomalous). The electric and magnetic components of seismo-associated electromagnetic fluctuation are estimated very faint, being some fraction of $mV/m(Hz)^{1/2}$ and some fraction of $nT/(Hz)^{1/2}$ or less, respectively (Parrot et al. (1993) and Sgrigna et al. (2007)). Moreover, the complexity of the lithosphere-atmosphere-magnetosphere coupling mechanism, asks for further studies in order to clearly distinguish anomalous signals from background noise and to asses their correlation with earthquakes occurrence (De Santis et al. (2015) and references therein). In order to infer the seismic signals in the electric field measurements, natural variations in the electric fields should be subtracted. In particular, it is relevant: the equatorial Electrojet (EEJ) (Alken and Maus, 2007), at the magnetic equator with an amplitude of the order of less than a mV/m, and the interplanetary electric field (IEF), a penetrating field that occurs especially when the interplanetary magnetic field turns negative with an amplitude of fraction of mV/m (Yamazaki and Maute, 2016). In addition, anthropogenic electromagnetic emissions as well as spurious fields induced by detector probe's intrinsic structure (Diego et al., 2017a), must be taken into account. In this framework, the study of precursors can take advantage from the continuous monitoring with repeated measurements in a short time period and high resolution performed by constellation of satellites such as the CSES missions and the three satellite of the Swarm mission (Olsen and Haagmansguest, 2006).

2. Space-borne measurements of the electric field

Measurements of electric fields in space plasma using the technique of double spherical probes installed on booms deployed from a spacecraft date back since 1960s. It was proposed from Aggson and Heppner (1964) for the ATS-4 satellite. The first successful results of this technique in a tenuous magnetospheric plasma was obtained onboard the S3-3 spacecraft in 1976 (Mozer et al., 1979), shortly followed by other experiments onboard GEOS-1 and ISEE-1 satellites in 1977. Afterwards, the use of crossed double probe systems in several satellite missions (such as GEOS-2 (Jones, 1978), Dynamic Explorer 2 (Maynard et al., 1981), Viking (Block et al., 1987), GEOTAIL (Tsuruda et al., 1994), Freja (Marklund et al., 1994), Polar (Harvey et al., 1995), Cluster (Gustafsson et al., 1997), C/NOFS (de La Beaujardiere, 2004), etc.) made possible measurements of the electric field vector components in the ionosphere and magnetosphere. These provided a direct knowledge of the electric field structure, also allowing a detailed correlation with the correspondent magnetic field configuration. Double probe sensors have been successfully used in the D, E, and F ionospheric regions, as well as in the

Table 1
Typical plasma conditions as measured by Swarm A satellite and corresponding equivalent impedance values adopted for test measurements on the EFD prototype. Note that, the value of the plasma-probe capacitance, calculated for an spherical probe (3 cm radius) using Swarm plasma data, is 19 pF, but due to the presence of the stubs, which shade part of the sensor surface, its value is reduced to about 12 pF.

Plasma conditions		Current Injected	Impedance Z_c	
Density	Temperature		Resistance	Capacitance
$2.5 \cdot 10^{11}\ m^{-3}$	2200 K	5 μA 10 μA	25 $k\Omega$ 14 $k\Omega$	$\simeq 12\ pF$

(a) Photograph of the sensor.

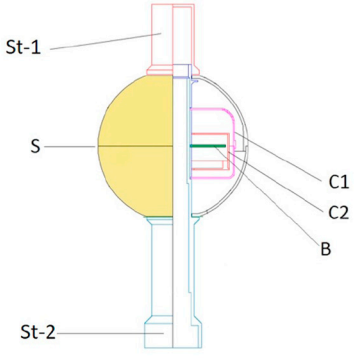

(b) Mechanical structure.

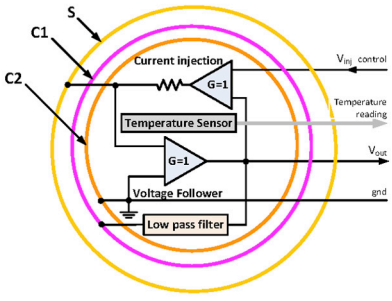

(c) Electronic Board.

Fig. 2. EFD probe. The yellow sphere S is the sensor current collector; the first inner hollow shell C1 is bootstrapped to the potential of the probe in order to minimize the capacitive coupling of the outer sphere with the ground. The stubs St1 and St2 are also connected to the bootstrap circuit in order to reduce boom perturbations by preventing disturbances to the sphere potential. The cylinder C2 is the shell connected to the ground and contains the electronic board B. In the block diagram (c) the simplified schematic of the electronics is shown. (For interpretation of the references to colour in this figure legend, the reader is referred to the Web version of this article.)